IEEE Access
Multidisciplinary | Rapid Review | Open Access Journal

Received August 16, 2017, accepted September 27, 2017, date of publication October 12, 2017,
date of current version November 7, 2017.

Digital Object Identifier 10.1109/ACCESS.2017.2761391

Energy Management for Distribution Networks Through Capacity Constrained State Optimization

SOHEL UDDIN, (Student Member, IEEE), OLAV KRAUSE, (Member, IEEE), AND DANIEL MARTIN, (Member, IEEE)

School of Information Technology and Electrical Engineering, The University of Queensland, Brisbane, QLD 4072, Australia

Corresponding author: Sohel Uddin (s.uddin@uq.edu.au)

This work was partially supported by the Australian Research Council through the Linkage Project LP150101006 Monitoring and Management System for Smart Distribution Networks.

ABSTRACT The widespread installation of distributed energy resources and demand side management resources into the distribution system has the potential to lead its operational parameters outside of their allowable limits. A standard strategy would be to increase the capacity of the network, however, this is costly. A cost-effective strategy could be to improve the management of such a system by improving the determination of its actual capacity. Recent advances in ICT equipment make it appear possible to manage the critical loading conditions instead of increasing capacity of the network. Thus, an energy management system is required to perform that function during the critical loading. In this paper, the authors present an approach for controlling network-oriented energy management systems on a distribution network using network capacity constraints. The proposed approach has been formulated in terms of linear inequality constraints. These constraints are derived from the functional relationships between an arbitrary set of control variables and an extensive variety of constrainable operational variables. The feasibility of the proposed constrained generation is demonstrated using linear programming, which performs the state optimization that already permits the usage of an extensive variety of cost functions. The significant feature of this approach is that it is flexible in terms of both constraint parameters and control variables. The proposed approach is demonstrated using an IEEE 13 bus distribution system.

INDEX TERMS Energy management, distribution systems, capacity constraints, linearization techniques, optimization.

I. INTRODUCTION

Conventional distribution systems (DS) have been designed to have a capacity adequate to meet the demand required at any time, where power flows in one direction to the consumer. Currently, the DS is being impacted by an increasing installation of different types of distributed energy resources (DER), such as photovoltaic and wind turbines [1], [2], as well as a wider range of emerging demand-side management (DSM) resources, e.g. battery storage and electric vehicles (EVs) [3]–[5]. With the proliferation of these systems, the DS are increasingly being put at risk of operation outside their safe operational limits, such as defined by the allowable range of voltage magnitudes and rated currents. With DS usually being operated passively, the usual approach for adapting to the new loading pattern is by network augmentation. This is not necessarily the most economical approach since the increased capacity incurs substantial expenditure while typically having relatively low utilization. Another possible approach is to manage the operation of DER and DSM, to ensure that voltages and line flow do not breach network limits. If the DER and DSM resources are properly managed, the operation of the network can be retained within safe operational limits, even with further loads, on the capacity of the existing network. This may involve reactive power management, voluntary load curtailment or deferral as well as temporary DER feed-in curtailment. To do this, an energy management system for DS is required. In part, these options are being considered for a wide range roll-out in many DS in form of time-of-use tariffs, non-unity power factor settings for DER, over-voltage

feed-in curtailment of DER, under-voltage load shedding, etc. Most of these options are perceived as interventions by the users and operators of the affected assets and require either an incentive or compensation to be paid, representing additional costs for the distribution system operator (DSO). Generally, each of these options represents different costs for the DSO and they may involve different technical parameters such as controlling active or reactive power. Finding the cost-optimal dispatch is beneficial both as a planning and technology selection tool, as well as, prospectively, an online management system.

State Estimation (SE) is an important tool in power system energy management [6], [7], allows the most probable internal state of the network to be determined. In this paper, the adaptive SE technique published in [8] to be used as this technique can work under-determined and over-determined situations while other techniques can work for over-determined situation only. One of the most challenging tasks in formulating the optimization problem is the representation of the capacity constraining operational limits on the individual network elements in the control variable domain. With the true shape of the capacity limits in the relevant domain having a very complex shape [9], one of the most promising options is to use linear approximates of the location and orientation of these limits.

Different types of grid related optimization, summarized under the term Optimal Power Flow (OPF), are documented in the literature for the distribution system network. A centralized AC OPF can be used to manage the thermal and voltage constraints [10], [11]. This management system can be achieved based on DG reactive power dispatch, generation curtailment and on-load tap changer coordinated control. On top of this, the selection of optimization technique has a strong impact on the ability to find the optimal dispatch solution. Numerous optimization techniques have been used extensively to solve the non-linear problems in OPF. Heuristics methods such as particle swarm optimization [12], genetic algorithm [13], artificial neural network [14] can be applied to solve OPF problems. Such techniques need 80-100 iterations to find a feasible solution, which can take an unsatisfactory duration to resolve [15]. Classical optimization techniques (e.g. linear programming (LP), quadratic, mixed integer linear programming) perform significantly better in regard of iteration [16]–[18]. The LP contains a linear cost function with continuous variables. This method is simple, reliable, and efficiently handles inequality constraints. Another key point, this method can achieve the optimal solution within a fewer number of iterations, whereas 80-100 iterations can take place with heuristic methods [19]–[21].

The purpose of this research is to develop a flexible, comprehensive framework to define and solve state optimization problems for as many scenarios as possible. In this framework, the key focus is to formulate how capacity constraining limits on operational parameters of individual network elements can be mapped onto an almost arbitrary set of control variables using the demonstrated linearization technique. In order to obtain this goal, the network should maximize its own utilization using the constraint, where the DG and DSM resources are treated as control parameters. The maximum utilization is achievable by optimizing the DG and DSM resources. For demonstrating of the validity purpose, the proposed approach is applied to IEEE 13 bus distribution network [22].

The main contribution of this paper is as follows:

1) To develop a comprehensive framework that allows to formulate a wide range of arbitrary combinations of controlled and constrained variables in Newton solvers, which include not only the traditional Newton-Raphson technique, but also the traditional WLMS state estimation. While OPF has been performed for a long time, most of its formulation is narrowly defined in the choice of constrainable operational parameters. In the OPF, more often than not very relevant operational parameters like branch currents cannot be constrained and so alternative, yet not equivalent, parameters like active power flows are used as replacements.

2) Some of the implementations popular in the research community use DC power flow formulations for the sensitivity analysis that required to formulate the capacity-related constraints on the nominated control variables. Our proposed implementations usually already include the partial derivatives that needed to formulate the constrained optimization problem as described in this paper. This means that it is also relatively easy to formulate a capacity constrained state optimization, constructed on an SE system and allowing real-time control.

3) In a real system, limits are needed on voltage, line current, imbalances etc. The system becomes too slow down due to the computational burden from incorporating every constraint into the model [23]. Thus a relatively flexible environment is required onto the systems where we can put any kind of constraints with arbitrary parameters on the constraints.

II. PROBLEM STATEMENT

The problem of OPF can be mathematically represented as follows

$$\min_{\mathbf{u}} \ f(\mathbf{u}) \tag{1}$$

$$\text{subject to } \mathbf{A} \cdot \mathbf{u} \leq \mathbf{b} \tag{2}$$

with

$$\mathbf{u}_{\min} \leq \mathbf{u} \leq \mathbf{u}_{\max} \tag{3}$$

where $\mathbf{u}, \mathbf{A}$ and $\mathbf{b}$ represent, respectively, the control variables, the coefficient matrix and the coefficient vector. Capacity constraints can be represented by an inequality (2). The constraints on control variable can be specified by inequality (3). The next section will focus on how to formulate the capacity constraint from linear inequality constraint and incorporate it with (1) to obtain the overall functionality for the OPF.

A. OPERATIONAL PARAMETERS

It is possible to model an n-bus distribution system as being under the influence of an input vector **i** including some control variable **u**. The operational state of the network can be represented as the complex voltage vector **x** (**i**) from which nominated operational parameters can be computed. These nominated operational parameters, or in short outputs can be represented by vector **o**(**i**), which cannot be measured directly, but has to be determined from **i** by either power flow analysis or state estimation, depending on the composition of **i**. For example, the input vector **i** in a Newton-Raphson power flow problem could be composed of magnitude of nodal voltage (V_i) at node i, respective phase angle of voltage (δ_i), reactive power (Q_i) and active power (P_i) as illustrated in (4). One example of a possible control vector could be the combination of both active and reactive power at any bus k as in (5). This could correspond to a four quadrant inverter coupled storage system.

The reason to choose PQ node as a controllable parameter is that we can usually control P and Q in a realistic DS scenario. It can be considered PV node as a controllable parameter where we can control P obviously but also needs to be adjusting the voltage set point of a system with an automatic voltage regulator. However, controlling of voltage set point is rarely performed in DS.

Basically, equations (4) and (5) can be written in one equation, but those are split here to better visualize.

$$\mathbf{i} = \begin{bmatrix} |V_1| \\ \delta_1 \\ \vdots \\ |V_i| \\ P_i \\ \vdots \\ \mathbf{u} \\ \vdots \\ P_n \\ Q_n \end{bmatrix} \tag{4}$$

$$\mathbf{u} = \begin{bmatrix} P_k \\ Q_k \end{bmatrix} \tag{5}$$

The internal state of a modeled network is a function of the given input **i** containing **u**. The internal state of the network is extract from SE. In this state all parameters of input vectors can be represented by the voltage magnitude and respective phase angle only.

$$\mathbf{x}(\mathbf{i}) = \begin{bmatrix} |V_1|(\mathbf{i}) \\ \delta_1(\mathbf{i}) \\ \vdots \\ |V_n|(\mathbf{i}) \\ \delta_n(\mathbf{i}) \end{bmatrix} \tag{6}$$

The SE will inform the simulation layer that is used by the optimizer to evaluate the impact of its control variables on the constrained output variables. From the simulation layer the assigned output vectors **o** (**i**) being as a function of **x** (**i**).

$$\mathbf{o}(\mathbf{i}) = \begin{bmatrix} o_1(\mathbf{x}(\mathbf{i})) \\ \vdots \\ o_m(\mathbf{x}(\mathbf{i})) \end{bmatrix} \tag{7}$$

The output vector **o** (**i**) is usually composed of non-linear, non-analytic, non-injective functions. In order to transform inequality constraints on **o** (**i**) into inequality constraints on **u**, a linearisation technique has used which described in the following section.

B. LINEARIZATION TECHNIQUE

The linearization system can be implemented mainly using three techniques, such as sampled sensitivity, Zbus matrix and analytically [24], [25]. The sampled based technique is easier to implement but processing time is slow, while the Zbus matrix method is the more precise linear model, but it is unable to capture non-linear behavior. The analytical method is challenging to implement but its processing time is very quick ensuring the maximum possible precision of linearization. In this paper, the analytical method will be implemented which is based on a Jacobian matrix. With the intention of generating linear inequality constraints on the control vectors from limits defined on nominated operational variables, a linearized model of the sensitivity of the bounded operational variables to changes of the control vectors is needed. To establish this linear map between control vectors and constraint variables, a linearization of both the non-linear functions are required involving input vectors with an internal state, and potentially non-linear functions involving constrained variables with state variables. Both linearizing can be formulated as the Jacobian matrix of the vectors of functions corresponding to provide input values and constraint variables respectively. With the Nabla operator ∇_v defined as (8), the Jacobian of the constrained variables functions can be calculated as in (9)

$$\nabla_v = \begin{bmatrix} \frac{\partial}{\partial e_1} \frac{\partial}{\partial f_1} \cdots \frac{\partial}{\partial e_n} \frac{\partial}{\partial f_n} \end{bmatrix} \text{ with } V_i = (e_i + j \cdot f_i) \tag{8}$$

$$\mathbf{J_o}(\mathbf{x}) = \mathbf{o}(\mathbf{x}) \cdot \nabla_v \tag{9}$$

where e_i and f_i represent the real and imaginary parts of the complex nodal voltage (V_i) respectively, at any node i. The index v in ∇_v indicates which variables are used and which need to be derived. The **o** (**x**) indicates the functional relationship between the constraint and state vector.

Complementing the provided non-linear input vector **i**, the functions involving the corresponding variables to the internal state vector **x** (**i**) are needed to linearize the non-linear relationship between the input and state vectors. So the Jacobian of the input vector functions can be calculated as in (10)

$$\mathbf{J_i}(\mathbf{x}) = \mathbf{i}(\mathbf{x}) \cdot \nabla_v \tag{10}$$

where **i** (**x**) represent the functional relationship between the input vector and state vector. Two main conditions must

be checked for the linearization process. Firstly, the overall linearization of the input vector may be either constant or controllable and secondly, all input vectors towards the output vector. As pointed out those two conditions, a linearization map is established between equations (9) and (10), as stated in (11).

$$\Delta \mathbf{o}(\Delta \mathbf{i}) = \mathbf{J}_{\boldsymbol{o}}(\mathbf{x}) \cdot \mathbf{J}_{\boldsymbol{i}}^{-1}(\mathbf{x}) \cdot \Delta \mathbf{i} \tag{11}$$

where $\mathbf{J}_{\boldsymbol{i}}^{-\mathbf{1}}(\mathbf{x})$ indicates the inverse matrix of $\mathbf{J}_{\boldsymbol{i}}(\mathbf{x})$

The inverse matrix is able to map only in a situation where the exactly defined case can happen. The inverse matrix does not exist if the system contains redundancy which would turn the system into a singularity. In that case, the system is not solvable. The adoption of a pseudo matrix instead of an inverse matrix is a solution that will provide a probable outcome, preventing this drawback. Therefore, the linearization map in (11) can be restated as (12). The details about pseudo matrix can be found in [9].

$$\Delta \mathbf{o}(\Delta \mathbf{i}) = \mathbf{J}_{\boldsymbol{o}}(\mathbf{x}) \cdot \mathbf{J}_{\boldsymbol{i}}^{\dagger}(\mathbf{x}) \cdot \Delta \mathbf{i} \tag{12}$$

where $\mathbf{J}_{\boldsymbol{i}}^{\dagger}(\mathbf{x})$ is the pseudo matrix of $\mathbf{J}_{\boldsymbol{i}}(\mathbf{x})$. It allows the use of under-determined input vectors as shown in [8]. The linear map can be simplified as follows

$$\mathbf{J}_{\boldsymbol{io}}(\mathbf{x}) = \mathbf{J}_{\boldsymbol{o}}(\mathbf{x}) \cdot \mathbf{J}_{\boldsymbol{i}}^{\dagger}(\mathbf{x}) \tag{13}$$

C. CAPACITY CONSTRAINTS GENERATION

For each optimization interval, the state of the physical network is assumed to not change and that the nature of the functions used in the input function vector adequately reflects the connected equipment's voltage-dependent behavior. Therefore, the input vector during the optimization will always contain zeros except for as indicated in (14)

$$\Delta \mathbf{i} = [0 \cdots 0 \cdots \mathrm{u}_1 \cdots \mathrm{u}_m \cdots 0]^{\mathrm{T}} \tag{14}$$

Therefore, $\mathbf{J}_{\boldsymbol{uo}}(\mathbf{x})$ can be defined as only the columns of $\mathbf{J}_{\boldsymbol{io}}(\mathbf{x})$ that correspond to control variables in $\mathbf{u}$. For all constrained variables $\mathbf{o}(\mathbf{i})$, there is an upper and lower limit as shown in (15). Collating all constrained variables and limits in vector form, this can be stated as in (15)

$$\mathbf{o}^{\min} \leq \mathbf{o}(\mathbf{i}) \leq \mathbf{o}^{\max} \tag{15}$$

where $\mathbf{o}(\mathbf{i})$ is unable to stated analytically which represents the whole estimation procedure. A first-order Taylor Series is used to state the linear constraints of outputs as approximated for a given expansion point $\mathbf{x}_0$. The expansion point can be found using (16)

$$\mathbf{o}(\mathbf{i}) = \mathbf{o}(\mathbf{i}_0 + \boldsymbol{\Delta}\mathbf{i}) \approx \mathbf{o}(\mathbf{i}_0) + \mathbf{J}_{\mathbf{io}}(\mathbf{x}_0) \cdot \Delta \mathbf{i} \tag{16}$$

With the limitations of (14)

$$\mathbf{o}(\mathbf{i}) = \mathbf{o}(\mathbf{i}_0 + \boldsymbol{\Delta}\mathbf{i}) \approx \mathbf{o}(\mathbf{i}_0) + \mathbf{J}_{\mathbf{uo}}(\mathbf{x}_0) \cdot \Delta \mathbf{u} \tag{17}$$

Substituting (17) into (15) results in a set of linear inequalities leading to (18)

$$\mathbf{o}^{\min} \leq \mathbf{o}(\mathbf{i}_{\mathrm{o}}) + \mathbf{J}_{\mathbf{uo}}(\mathbf{x}_0) \cdot \Delta \mathbf{u} \leq \mathbf{o}^{\max} \tag{18}$$

Subtracting the expansion point of the operational values in (18) leads to (19) to transform the set of linear inequalities which is equivalent to (2),

$$\mathbf{o}^{\min} - \mathbf{o}(\mathbf{i}_{\mathbf{o}}) \leq \mathbf{J}_{\boldsymbol{uo}}(\mathbf{x}_{\mathbf{0}}) \cdot \Delta \mathbf{u} \leq \mathbf{o}^{\max} - \mathbf{o}(\mathbf{i}_{\mathbf{o}}) \tag{19}$$

This expression can then be split up into lower and upper limits resulting in the following inequality constraints

$$\begin{bmatrix} \mathbf{J}_{\boldsymbol{uo}}(\mathbf{x}_{\mathbf{0}}) \\ -\mathbf{J}_{\boldsymbol{uo}}(\mathbf{x}_{\mathbf{0}}) \end{bmatrix} \cdot \Delta \mathbf{u} \leq \begin{bmatrix} \mathbf{o}^{\max} - \mathbf{o}(\mathbf{i}_{\mathbf{o}}) \\ -\mathbf{o}^{\min} + \mathbf{o}(\mathbf{i}_{\mathbf{o}}) \end{bmatrix} \tag{20}$$

For all technically sensible setups and for $\mathbf{o}_{\mathbf{u}}^{\max} > \mathbf{o}_{\mathbf{u}}^{\min} \forall i \in \{1, \mathrm{m}\}$, the feasible region bounded by (20) is convex, but not necessarily closed. To ensure a closed feasible region, as well as to adequately reflect the operational limits of equipment being modeled by the control variables, the control variables themselves need to be constrained as well. Similar to (15) this control variable constraint on $\Delta \mathbf{u}$ can be formulated as in (21).

$$\mathbf{u}^{\min} \leq \mathbf{u}_0 + \Delta \mathbf{u} \leq \mathbf{u}^{\max} \tag{21}$$

Similar to the constraints on operational variables $\mathbf{o}(\mathbf{i})$, this can be restated as (22) to comply with (4)

$$\begin{bmatrix} \mathbf{I} \\ -\mathbf{I} \end{bmatrix} \cdot \Delta \mathbf{u} \leq \begin{bmatrix} \mathbf{u}^{\max} - \mathbf{u}_0 \\ -\mathbf{u}^{\min} + \mathbf{u}_0 \end{bmatrix} \tag{22}$$

Combining (21) and (22) to (23) states linearly approximating the close feasible region where the constraints are closely convex [9].

$$\begin{bmatrix} \mathbf{J}_{\boldsymbol{uo}}(\mathbf{x}_{\mathbf{0}}) \\ -\mathbf{J}_{\boldsymbol{uo}}(\mathbf{x}_{\mathbf{0}}) \\ \mathbf{I} \\ -\mathbf{I} \end{bmatrix} \cdot \Delta \mathbf{u} \leq \begin{bmatrix} \mathbf{o}^{\max} - \mathbf{o}(\mathbf{i}_{\mathrm{o}}) \\ -\mathbf{o}^{\min} + \mathbf{o}(\mathbf{i}_{\mathrm{o}}) \\ \mathbf{u}^{\max} - \mathbf{u}_0 \\ -\mathbf{u}^{\min} + \mathbf{u}_0 \end{bmatrix} \tag{23}$$

The proposed approach can be implemented for a wide range of capacity constraints such as voltage constraints, line current, active and reactive power etc. Here, to demonstrate its validity, the presented approach has been verified for voltage constraints. Moving on now to consider voltage as capacity constraint, the inequality (23) can be restated as follows

$$\begin{bmatrix} \mathbf{J}_{\boldsymbol{uo}}(\mathbf{x}_{\mathbf{0}}) \\ -\mathbf{J}_{\boldsymbol{uo}}(\mathbf{x}_{\mathbf{0}}) \\ \mathbf{I} \\ -\mathbf{I} \end{bmatrix} \cdot \Delta \mathbf{u} \leq \begin{bmatrix} \mathbf{V}^{\max} - \mathbf{V}(\mathbf{i}_{\mathrm{o}}) \\ -\mathbf{V}^{\min} + \mathbf{V}(\mathbf{i}_{\mathrm{o}}) \\ \mathbf{u}^{\max} - \mathbf{u}_0 \\ -\mathbf{u}^{\min} + \mathbf{u}_0 \end{bmatrix} \tag{24}$$

Following this, the control variables can be either an arbitrary set of active power/reactive power or a combination of both. In the presence of both active and reactive power, the inequality (24) can be expressed as

$$\begin{bmatrix} \mathbf{J}_{(\boldsymbol{Po},\boldsymbol{Qo})}(\mathbf{x}_{\mathbf{0}}) \\ -\mathbf{J}_{(\boldsymbol{Po},\boldsymbol{Qo})}(\mathbf{x}_{\mathbf{0}}) \\ \mathbf{I} \\ -\mathbf{I} \end{bmatrix} \cdot \begin{bmatrix} \Delta \mathbf{P} \\ \Delta \mathbf{Q} \end{bmatrix} \leq \begin{bmatrix} \mathbf{V}^{\max} - \mathbf{V}(\mathbf{i}_{\mathrm{o}}) \\ -\mathbf{V}^{\min} + \mathbf{V}(\mathbf{i}_{\mathrm{o}}) \\ \mathbf{P}^{\max} - \mathbf{P}_0 \\ \mathbf{Q}^{\max} - \mathbf{Q}_0 \\ -\mathbf{P}^{\min} + \mathbf{P}_0 \\ -\mathbf{Q}^{\min} + \mathbf{Q}_0 \end{bmatrix} \tag{25}$$

D. OPTIMIZATION TECHNIQUE

The inequality stated in (23) defines a constraint satisfaction problem, which for realistic and solvable cases will usually have an infinite number of probable solutions. An objective function is required to find the optimal solution which represents the most efficient use of the network capacity. A variety of cost functions is available in the literature which can be used with the presented algorithm. For simplicity, the LP based optimization is chosen here, as defined in (26). The proposed generated constraints are linear, which is another vital reason to choose LP because it is very efficient with a linear constraint. The LP is specialized for accomplishing economic dispatch in power network. This method is simple, reliable, efficient handling of inequality constraints. In addition, it has excellent convergence features and requires less computation time.

$$\mathbf{c}\,(\mathbf{i}) = \begin{bmatrix} c_1 \\ \vdots \\ c_n \end{bmatrix}^{\mathrm{T}} \cdot \mathrm{abs}\left\{ \begin{bmatrix} \Delta \mathbf{u}_1 \\ \vdots \\ \Delta \mathbf{u}_n \end{bmatrix} \right\} \begin{cases} \textit{Subject to} \\ \textit{inequality (23)} \end{cases} \tag{26}$$

where $\mathbf{c}\,(\mathbf{i})$ is the cost function, $c_1 - c_n$ are the incremental cost vector of the respective control variables $\mathbf{u}_1 - \mathbf{u}_n$ respectively.

The cost function as discussed above generally allows for all control variables to be used. The controllable reactive power can be formulated conservatively using (26). When there is an excess of active power, the customers either pay to receive this power or are rewarded if delivering power. Thus, it must be split non-conservatively by allowing active power flow in both directions. Therefore, this would allow the degree of freedom in a situation whereas increasing demand with decreasing generations, or decreasing demand with increasing generations. So it is easily possible to reward if there have an increased consumption. The equation (26) can be rewritten in the presence of both active and reactive power as in (27)

$$\mathbf{c}\,(\mathbf{i}) = \begin{bmatrix} c_1 \\ \vdots \\ c_t \end{bmatrix}^{\mathrm{T}} \cdot \begin{bmatrix} \Delta \mathbf{P}_1 \\ \vdots \\ \Delta \mathbf{P}_t \end{bmatrix} + \begin{bmatrix} c_{(n-t)} \\ \vdots \\ c_n \end{bmatrix}^{\mathrm{T}} \cdot \mathrm{abs}\left\{ \begin{bmatrix} \Delta \mathbf{Q}_{(n-t)} \\ \vdots \\ \Delta \mathbf{Q}_n \end{bmatrix} \right\} \begin{cases} \textit{Subject to} \\ \textit{inequality (25)} \end{cases} \tag{27}$$

An iterative method has been applied, as shown in the flowchart in Fig. 1, to minimize any linearization error from using (23) being subject to linearization error. The presented approach converges to the optimal solution by recalculating (23).

III. TEST NETWORK

The IEEE 13 bus distribution system [22] was used to demonstrate the proposed algorithm as the reference test case, with the network topology shown in Fig. 2. Node 650 is modeled as a reference node while all other nodes are constant power type load nodes.

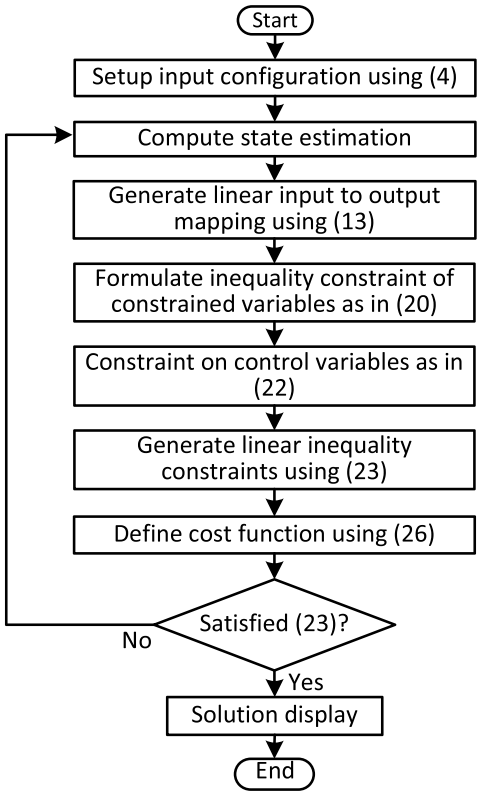

FIGURE 1. Framework of constraints with LP solution.

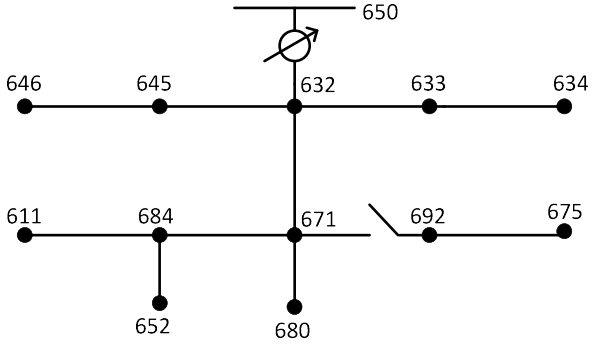

FIGURE 2. IEEE 13 bus distribution network [22].

All calculations are performed using per unit (p.u.) values, and consequently, the results will also be presented in p.u. In this test network, DSM resources and compensation devices are assumed to be available at certain nodes. The switch between nodes 671 and 692 is assumed as being closed. Additionally, the following modifications have been made compared to the original reference network as published in [22].

1) All branches are based on the positive sequence parameters only, with no parameter asymmetry among different phases and the neutral conductor.
2) All simulations are carried out on a single-phase equivalent circuit model and all three phase active and reactive power values are summed as a nodal total.
3) Mutual inductance has been neglected.

The following three demonstration cases are studied using this test network to demonstrate the validity of the proposed approach:

1) A compensation device with controllable reactive power installed at node 671
2) A compensation device at node 671 and two DSM facilities (e.g. EVs) with controllable active power at nodes 645 and 675
3) Price bidding scheme with two EVs at nodes 645 and 675, and compensation device at node 671

IV. CASE STUDY RESULT AND DISCUSSION

The proposed approach can be used with a wide range of operational constraints e.g. nodal voltage, line current etc. Here, for simplicity and to demonstrate the specific relevance of the constraints, the presented approach has been verified using only voltage constraints. For all buses, the limits of the system's lower and upper voltages were set to 0.95 p.u. and 1.05 p.u. The active and reactive power at the specified nodes is considered as the controllable parameter. Based on these constraints, the three cases mentioned in section III were investigated in the following sections.

A. CASE 1

A compensation device is installed at node 671, which is capable of sinking and sourcing reactive power at this node. The location of the compensation device was selected as it appears to be a likely choice in a real network management scenario. This is assumed to be the case for its location towards the end of the feeder and it is likely relatively balanced impact on the voltage in both branch-off, leading to node 611 and 675, respectively. The compensation device does not only influence the voltage at the bus it has been connected to, but also significantly affects voltages at other nodes of the network. With respect to voltage, three different main general conditions can arise within this network. These are voltage band violations due to under voltage (>0.95), voltage band violations due to over voltage (<1.05), and no voltage band violations (0.95-1.05). In theory, there can also be conditions when under and over voltage related violations occur at the same time. But since these are expected to be very rare, the proposed algorithm is demonstrated for the above mentioned three scenarios only.

1) UNDER VOLTAGE VIOLATION

At first, a scenario was considered where under voltage violation occurs. The base case for this scenario has been designed to produce a severe under voltage, with the voltage at all buses as shown in Fig. 3. The base case represents the operational conditions within the network without any control. In this figure, the base case voltage is indicated using blue, while red is used to show the proposed technique, and the constraint activation using green. Fig. 3 reveals that the lower voltage constraint (0.95) is activated at node 652 using the proposed technique, while all other nodes remain within the allowable limit. This indicates that the proposed approach

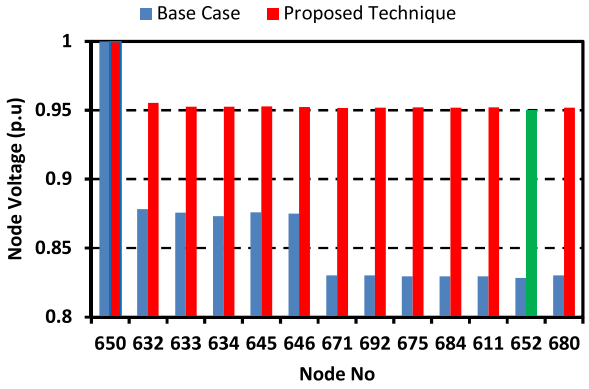

FIGURE 3. Bus voltage profile for under voltage violation.

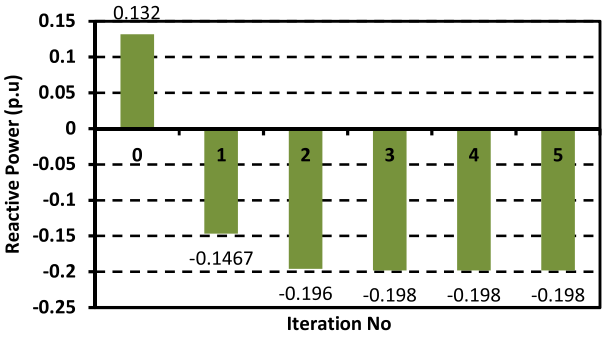

FIGURE 4. Optimized reactive power at node 671.

is able to mitigate the under voltage problem throughout the network, and is able to determine the minimal intervention required to return all nodal voltages to within statutory limits. The controllable reactive power compensation device installed at node 671 plays a vital role to eliminate the under voltage problem. The compensation device not only is improving the voltage profile at that particular node, but has also raised the voltage at the other nodes by optimizing their reactive power contribution. A particular node may need to either source or sink reactive power during optimization. Fig. 4 illustrates the converging set-point of the controllable reactive power at node 671 in the different iteration steps of the optimization. The horizontal axis in Fig. 4 represents the number of iteration (iteration no 0 refers to the base case) required to converge to the optimal solution, while the vertical axis displays the per unit controllable reactive power sourcing/sinking of the compensation device at the particular node. From Fig. 4, the optimized reactive power is negative (load indexed positively); the reason is that the proposed approach calculates that this node needs to source more reactive power to maintain entire network's voltage within the allowable limits. Initially, the particular node is sinking (represented by positive) 0.132 p.u. reactive power. At that time, according to this technique, reactive power must be sourced, rather than sunk, to return the voltage level to between 0.95 and 1.05 p.u. After this adjustment, a simulation is run to evaluate the likely impact of the updated reactive power set-point on the

network's operational state. Furthermore, the solution to this simulation, which is assumed to lie closer to the optimum solution, is then used to generate an updated linearization and to re-state the capacity constraining equality constraints. Repeating this process, allows the optimization to converge into its final solution quickly, which in this case 0.198 p.u. reactive power to manage the voltage limits of the whole network.

Another key point is the low number of iterations needed for this technique to converge to the optimum state which returns all nodal voltages to within the required voltage band. To illustrate this, not only with the allocated reactive power at node 671, but also with the voltage values at nodes within the network, Fig. 5 shows the convergence of the voltage at node 652. It is observed from Fig. 5 that the approach presented in this paper reached the tolerable voltage magnitude in the third iteration. This demonstrates an advantage of using the proposed technique of classical constrained optimization using linear inequality constraints, representing capacity constraints and generated using a linearized network model, over heuristic methods that may need 80-100 iterations to arrive at the solution [19]–[21]. Furthermore, the aim of the objective function is to minimize the cost of the system with all constraints observed to get the optimal solution. The cost function value for each iteration during optimization is listed in Table 1. The cost of reactive power compensation at node 671 has been set to \$0.2/p.u. From the table, the final cost function is 0.1188, which is achieved on the third iteration.

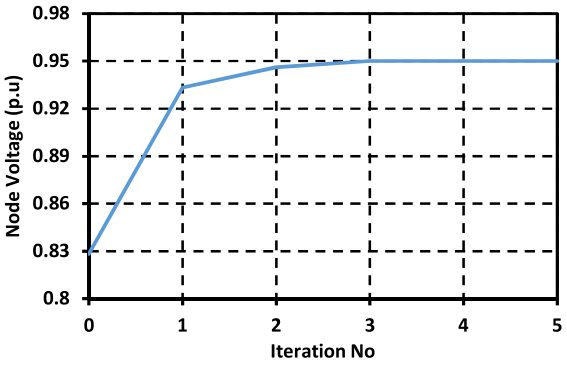

FIGURE 5. Voltage convergence property with iteration at node 652.

TABLE 1. Cost function value of control variable for under voltage violation.

Iteration no	Price of Q at node 671 (\$/p.u)	Cost function value
1		0.088
2		0.1182
3	0.2	0.1188
4		0.1188
5		0.1188

2) OVER VOLTAGE VIOLATION

This section demonstrates the proposed technique in a scenario with an over-voltage violation. The bus voltage profile

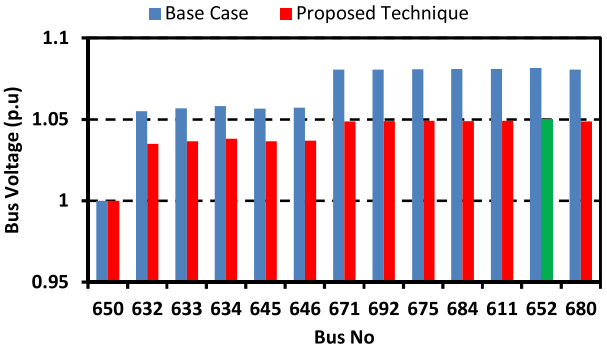

FIGURE 6. Bus voltage profile for over voltage violation.

of the network is shown in Fig. 6. Similarly to the previous scenario, the compensation device is installed at node 671. As indicated in green in Fig. 6, the upper voltage constraint (1.05) is activated at node 652, and that the voltage of all the other nodes remains within the permissible range. It takes four iterations to converge to the optimal solution. Unlike the previous scenario, the available compensation device at node 671 sinks some reactive power to bring back voltage of all buses within the permissible limit. The cost function value is 0.1145 when the price of reactive power at node 671 is kept same as the previous scenario.

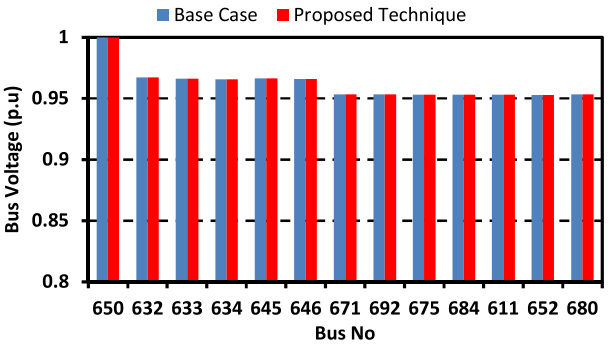

FIGURE 7. Bus voltage profile for no violation.

3) NO VIOLATION

As avoiding unnecessary activation is a key feature of a deployable network management system, the third scenario demonstrates this unnecessary behavior using the proposed technique when there is no voltage band violation throughout the network. No voltage constraint is reached at any node of the network, and hence all the voltages remain within the permissible limits as in Fig 7. The voltage at all buses is the same in both the base case and when the proposed technique is applied to under and over voltage scenarios. The compensation device continues to idle because no change is needed to correct the network state. As a result, there is no cost function associated with this scenario. The controllable compensation device would start source/sink reactive power when this is necessary. The main achievement of this approach is that

the reactive power starts working only when necessary. It is clearly seen that the presented approach prevents the network from over and under voltage conditions.

B. CASE 2

The proposed approach successfully manages the voltage constraints throughout the entire network using reactive power control, as described in the previous case. It is also possible to manage the voltage constraints in the presence of DSM resources, i.e. with the control of EVs or storage. The active power needs to be included as a control parameter in the system for DSM resources.

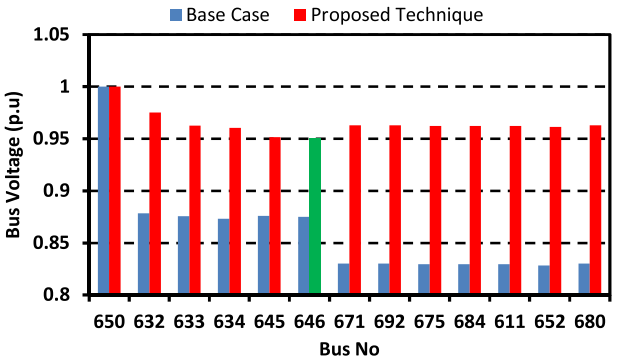

FIGURE 8. Bus voltage profile for case 2.

TABLE 2. Active and reactive power sharing at controllable nodes for case 2.

Sink active power, P (p.u)		Source reactive power (Q) at node 671 (p.u)
node 645	node 675	
0.39	0.148	0.4

A case was considered where the EVs are available to the network, in addition to the compensation device already discussed in the previous case. The compensation device remains installed at node 671 along with the available two EVs at nodes 645 and 675. The EVs are capable of sinking active power in an interval from zero to the maximum power. The EVs are treated as a consumer at this particular node. It is worth mentioning that the cost function in the presented approach generally rewards if the active power is being sourced to the network and penalized when sinking the active power from the network. The reward of the cost function refers to negative cost as explained in (27). The voltage profile of the network is shown in Fig. 8. The lower voltage band constraint is activated at node 646 while the voltage of other nodes satisfies the constraint. The compensation device at node 671 sources reactive power to bring back the network voltage within the allowable limit as recorded in Table 2. The EVs sink active power once the compensation device reaches its maximum value. Or stated differently, the presented technique determinates that no charging can be allowed unless voltage values are returned to within required limits. Using the available reactive power sources is an economical way to support charging by the EVs balancing available reactive power with the allowable charging active power to allow for the maximum charging power possible under the given constraints. This is an essential capability of a network management system and demonstrates the cross-domain applicability of the presented technique. The amount of active power sunk by both EVs is given in Table 2.

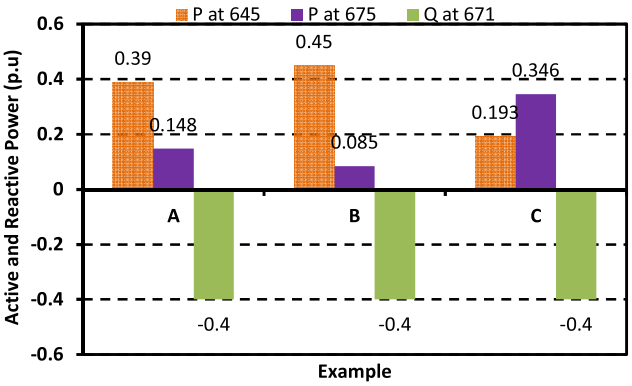

FIGURE 9. Active and reactive power allocation at controllable nodes for different scenario.

TABLE 3. Bidding price of consumers.

Example	Active power price ($/p.u)		Reactive power price at node 671 ($/p.u)
	Node 645	Node 675	
A	1	1	0.2
B	1	0.7	0.2
C	0.7	1	0.2

C. CASE 3

The last case presented is the demonstration of the applicability of the presented technique to a more complex price bidding scheme. Similar to the previous case, two consumers have controllable active power at nodes 645 and 675, and a compensation device is placed at node 671. The controllable active power for both consumers has been set with an interval between zero and 0.45 p.u to represent the EVs. The controllable reactive power for the compensation device at node 671 is set to 0.4 p.u. Three examples have been considered to demonstrate the price bidding scheme, as shown in Table 3. From this table it is assumed that both consumers are willing to pay one dollar p.u. in example A. The price of reactive power has been set to be lower than the active power because the reactive power compensation device is cheaper than supplying active power. Thus, the approach will prioritize the transfer of reactive power. This leads to the behavior as shown by example A in Fig. 9. The consumer at node 645 is receiving 0.39 p.u. of active power, which is almost 86.7% of its maximum capacity. The consumer at

node 675 is receiving only 0.148 p.u. of active power, which is 32.9% of that required. From Fig. 2, node 675 is located at the far end of the network. Thus, the consumer at this point will not receive the desired power. This behavior is a consequence of the linear cost function where power delivery to all consumers is evaluated equally, thus the optimizer trying to maximize overall power delivery.

A different scenario is illustrated by example B in the same figure. This is the active power allocation considering the network operator is allowing consumers to compete for the available transfer capacity by bidding at different prices for their power delivery. In this particular example, we assume that the consumer at node 645 is willing to pay a significantly higher price for the delivery of active power than the consumer at node 675 (see Table 3). It is clear from the figure that the node 645 is taking its maximum power while the node 675 is getting only 18.8% (0.085p.u) of its required. The example C in the figure is also showing the same phenomenon where the consumer at node 675 is getting the maximum power as it offers more money than other. The cost function value for all three examples is listed in Table 4. From the table, the overall cost function value is higher when both consumers are bidding the same price.

TABLE 4. Cost function value of control variables for case 3.

Example	Cost function value
A	0.327
B	0.239
C	0.245

Several scenarios have investigated by putting EVs and multiple compensation devices at a different location in the network. All scenarios have shown the same behavior as in Fig. 9, which will be presented in a follow-up paper. These extreme scenarios pose a question for which there is no purely technical answer. In both extreme cases either everybody is forced to bid at the same price or has the ability to outbid others, likely leading to concerns about the fairness of the allocation. Everybody is forced to bid at the same price will lead to a technically optimal allocation, but not necessarily to the economically optimal allocation. The other extreme will arguably lead to the economically optimal allocation, which can clearly be seen not to be the technically optimal one in most cases. A discussion is therefore required on how society and consumers want the network to behave, what an acceptable concept of fairness in the presence of network capacity constraints will look like, and how to codify this in mathematical terms. This is beyond this paper, which is on presenting a technique that allows such systems to be implemented and operated at computational costs superior to often used heuristic approaches.

V. CONCLUSION

In this article, a general technique for the realization of capacity constrained network state optimization, intended for use in real-time network-oriented energy management systems, has been described and demonstrated in a number of different, plausible, scenarios. Despite having been presented using linear cost functions only, the general approach is applicable to a much wider range of objective functions and other optimality defining models (such as markets). It is demonstrated and explained how the linear inequality constraints can be mapped from a variety of operational parameters that are related to the arbitrary set of control variables. It was found that this approach is able to manage the distribution systems operational parameters (e.g. voltage problem) in the presence of DER and DSM resources by utilizing network's own capacity. Furthermore, it was found that this approach has supreme convergence behavior; by far out-performing frequently used heuristic techniques. Moreover, it is applicable in complex scenarios including multi-domain scenarios and price bidding environments. From the market structure (e.g. price bidding) perspective, it was shown that the arrival of autonomous network management systems raises questions beyond mere practicality and viability of solutions, but there is a need for the discussion and mathematical codification of social concepts such as fairness.

ACKNOWLEDGMENT

The authors would like to thank Dr Nahid - Al - Masood from the University of Queensland to improve the quality of this paper.

REFERENCES

[1] W. Sheng, K.-Y. Liu, and S. Cheng, "Optimal power flow algorithm and analysis in distribution system considering distributed generation," *IET Generat., Transm. Distrib.*, vol. 8, no. 2, pp. 261–272, 2014.

[2] H.-G. Yeh, D. F. Gayme, and S. H. Low, "Adaptive VAR control for distribution circuits with photovoltaic generators," *IEEE Trans. Power Syst.*, vol. 27, no. 3, pp. 1656–1663, Aug. 2012.

[3] P. Papadopoulos, S. Skarvelis-Kazakos, I. Grau, L. M. Cipcigan, and N. Jenkins, "Electric vehicles' impact on British distribution networks," *IET Elect. Syst. Transp.*, vol. 2, no. 3, pp. 91–102, 2012.

[4] S. Taira, Z. Ziadi, and T. Funabashi, "Assessment of impact of distributed generators, plug-in electric vehicle and battery energy storage system on power distribution losses," in *Proc. 1st Int. Future Energy Electron. Conf. (IFEEC)*, Nov. 2013, pp. 675–680.

[5] I. Wasiak, R. Pawelek, and R. Mienski, "Energy storage application in low-voltage microgrids for energy management and power quality improvement," *IET Generat., Transmiss. Distrib.*, vol. 8, no. 3, pp. 463–472, Mar. 2014.

[6] Y.-F. Huang, S. Werner, J. Huang, N. Kashyap, and V. Gupta, "State estimation in electric power grids: Meeting new challenges presented by the requirements of the future grid," *IEEE Signal Process. Mag.*, vol. 29, no. 5, pp. 33–43, Sep. 2012.

[7] V. Kekatos and G. B. Giannakis, "Distributed robust power system state estimation," *IEEE Trans. Power Syst.*, vol. 28, no. 2, pp. 1617–1626, May 2013.

[8] O. Krause and S. Lehnhoff, "Generalized static-state estimation," in *Proc. 22nd Austral. Univ. Power Eng. Conf. (AUPEC)*, 2012, pp. 1–6.

[9] O. Krause, S. Lehnhoff, E. Handschin, C. Rehtanz, and H. F. Wedde, "On feasibility boundaries of electrical power grids in steady state," *Int. J. Elect. Power Energy Syst.*, vol. 31, no. 9, pp. 437–444, 2009.

[10] S. Bruno, S. Lamonaca, G. Rotondo, U. Stecchi, and M. L. Scala, "Unbalanced three-phase optimal power flow for smart grids," *IEEE Trans. Ind. Electron.*, vol. 58, no. 10, pp. 4504–4513, Oct. 2011.

[11] Y. Cao, Y. Tan, C. Li, and C. Rehtanz, "Chance-constrained optimization-based unbalanced optimal power flow for radial distribution networks," *IEEE Trans. Power Del.*, vol. 28, no. 3, pp. 1855–1864, Mar. 2013.
[12] M. A. Abido, "Optimal power flow using particle swarm optimization," *Int. J. Elect. Power Energy Syst.*, vol. 24, no. 7, pp. 563–571, 2002.
[13] D. Devaraj and B. Yegnanarayana, "Genetic-algorithm-based optimal power flow for security enhancement," *IEE Proc.-Generat., Transmiss. Distrib.*, vol. 152, no. 6, pp. 899–905, Nov. 2005.
[14] J. N. Fidalgo and J. A. P. Lopes, "Forecasting active and reactive power at substations' transformers," in *Proc. IEEE Bologna Power Tech Conf.*, vol. 6. Jun. 2003, p. 6.
[15] P. Pezzini, O. Gomis-Bellmunt, and A. Sudrià-Andreu, "Optimization techniques to improve energy efficiency in power systems," *Renew. Sustain. Energy Rev.*, vol. 15, no. 4, pp. 2028–2041, 2011.
[16] M. R. AlRashidi and M. E. El-Hawary, "Hybrid particle swarm optimization approach for solving the discrete OPF problem considering the valve loading effects," *IEEE Trans. Power Syst.*, vol. 22, no. 4, pp. 2030–2038, Nov. 2007.
[17] R. Dai and M. Mesbahi, "Optimal power generation and load management for off-grid hybrid power systems with renewable sources via mixed-integer programming," *Energy Convers. Manage.*, vol. 73, pp. 234–244, Sep. 2013.
[18] T. Dhadbanjan and S. S. K. Vanjari, "Linear programming approach for power system state estimation using upper bound optimization techniques," *Int. J. Emerg. Electr. Power Syst.*, vol. 11, no. 3, pp. 1–18, 2010.
[19] I. J. Hasan, M. R. A. Ghani, and C. K. Gan, "Optimum distributed generation allocation using PSO in order to reduce losses and voltage improvement," in *Proc. 3rd IET Int. Conf. Clean Energy Technol. (CEAT)*, 2014, pp. 1–6.
[20] N. Nikmehr and S. N. Ravadanegh, "Heuristic probabilistic power flow algorithm for microgrids operation and planning," *IET Generat., Transm. Distrib.*, vol. 9, no. 11, pp. 985–995, 2015.
[21] K. Vaisakh, P. Praveena, and S. R. M. Rao, "Solving optimal power flow problems using bacterial swarm optimization algorithm," in *Proc. 8th Int. Conf. Adv. Power Syst. Control, Operat. Manage. (APSCOM)*, 2009, pp. 1–7.
[22] IEEE Power Engineering Society, USA. (2009). *IEEE 13 Node Test Feeder*. [Online]. Available: http://ewh.ieee.org/soc/pes/dsacom/testfeeders/index.html
[23] H. Wang, C. E. Murillo-Sanchez, R. D. Zimmerman, and R. J. Thomas, "On computational issues of market-based optimal power flow," *IEEE Trans. Power Syst.*, vol. 22, no. 3, pp. 1185–1193, Aug. 2007.
[24] S. V. Dhople, S. S. Guggilam, and Y. C. Chen, "Linear approximations to AC power flow in rectangular coordinates," in *Proc. 53rd Annu. Allerton Conf. Commun., Control, Comput. (Allerton)*, 2015, pp. 211–217.
[25] L. S. Jonas Persson, "Comparison of three linearization methods," in *Proc. Power Syst. Comput. Conf.*, Glasgow, Scotland, Jan. 2008, pp. 1–7.

SOHEL UDDIN received the B.Sc. degree in electrical and electronic engineering from the Khulna University of Engineering and Technology, Khulna, Bangladesh, in 2009, and the M.Sc. degree in electrical, electronic and systems engineering from Universiti Kebangsaan Malaysia, Malaysia, in 2013. He is currently pursuing the Ph.D. degree with The University of Queensland (UQ), Australia. Prior to joining UQ, he served with the Department of Electrical Engineering, University of Malaya, Malaysia, as a Research Assistant, from 2013 to 2014. His research interests include the estimation of operational state of distribution networks, energy management of distribution networks, and power quality.

OLAV KRAUSE (M'15) received the Ph.D. degree in engineering science from TU Dortmund University, Dortmund, Germany, in 2009. He was a Research Associate for five years, in 2009 on the topic usage potential of distribution networks. He is currently the T&R Lecturer with The University of Queensland, Brisbane, QLD, Australia; a fellow of the Hanse-Wissenschaftskolleg-Institute for Advanced Studies, Delmenhorst, Germany; and a Research Fellow of the National Natural Science Foundation of China . His current research interests are the estimation of operational state of distribution networks from heterogenic measurement data and the determination of their remaining transfer capability. Neighboring topics are probabilistic calculus in power system analysis and distributed energy management.

DANIEL MARTIN (M'12) received the B.Eng. degree in electrical and electronic engineering (with study abroad in Germany) from the University of Brighton, Brighton, U.K., in 2000, and Ph.D. degree in electrical insulation from The University of Manchester, Manchester, U.K., in 2008. He investigated the suitability of using vegetable oils and synthetic esters as substitutes for mineral oil within large power transformers, and graduated in 2008. He then joined Monash University, Melbourne, VIC, Australia, where he was involved in transformer condition monitoring, quickly assuming the directorship of the Centre for Power Transformer Monitoring. At the beginning of 2013, he moved to The University of Queensland, Brisbane, QLD, Australia, where he was involved in a transformer condition monitoring project funded by the local utilities.